# Particle Physics Detectors
## or
## Experimental Electrodynamics

- Elementary particles are detected via their
  interaction with matter
- Mainly electromagnetic interactions:
  ionization and excitation of matter
- “Applied QED”, but lots of other
  interesting physics involved

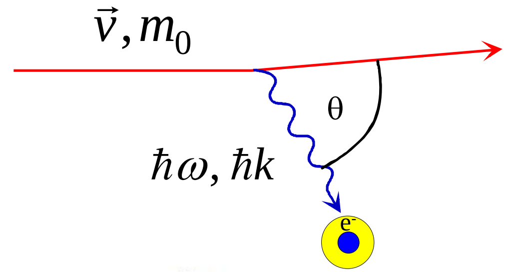


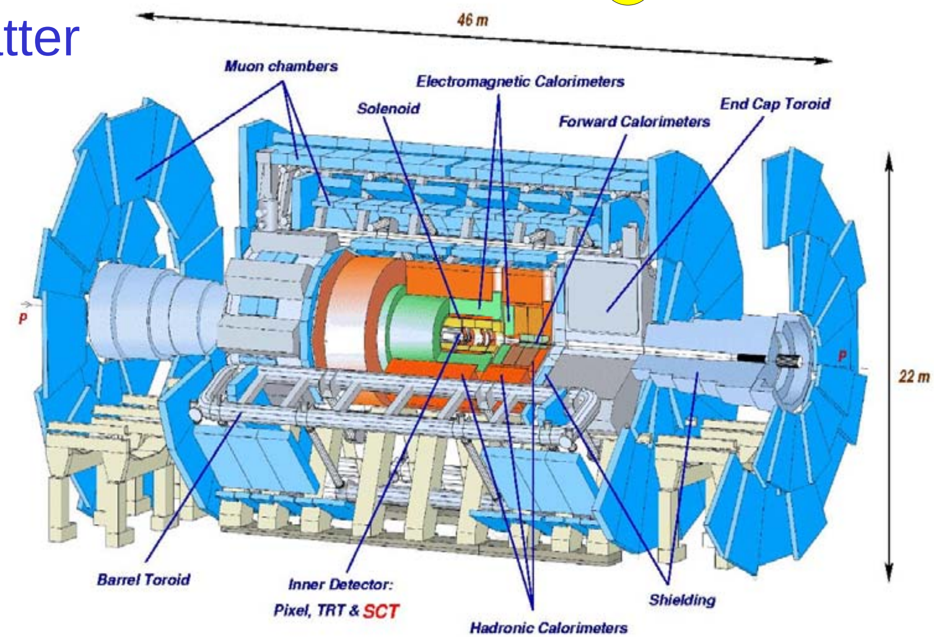


particle physics detectors today
are the biggest microscopes in the world
looking into the smallest structures


SUPA Graduate Lecture, Oct 2010

Stephan Eisenhardt

# Outline

- Classic detectors
- Detector concepts

lecture 1

- Interaction with matter

lecture 2

- Tracking detectors

lecture 3

- Photon detection

lecture 4

- Calorimeters

lecture 5

- Particle identification
- Trigger concepts

lecture 6

- Modern detectors

not presented

each new sensor technology increases our experimental reach

extension of our senses:

sense of touch

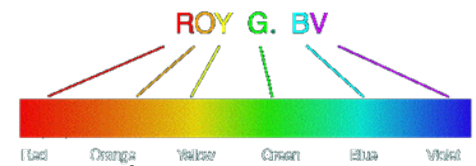


visual sense
heat sense
smell

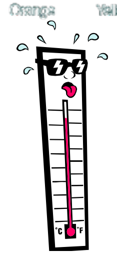

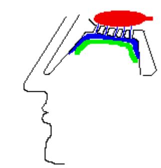

every increase in experimental reach opens a window for new insight into the structure of the world

# Classic Detectors

new techniques provided new insight ⟺ physics needs drove development

classic experiments defined our modern picture of the fundamental principles

- Measured parameters:
  - particle multiplicity (prong number)
  - vertex position
  - decay angles
  - ionisation of track
  - track curvature in mag. field
  - radius
  - photon production
  - charge production
  - time
- Derived parameters
  - momentum
  - energy loss / deposition
  - kinetic energy
  - particle ID (hypothesis)
  - velocity
- Particle properties
  - mass
  - charge
  - angular momentum
  - spin
  - helicity
  - life time / decay width
  - decay channels
- Process properties
  - cross-section
  - branching ratios
  - symmetry conservation

these basic parameters remain the same today…

# Cloud Chamber

invented 1929-31(?) by Wilson
(born in Edinburgh)

Anderson 1933

- "Wilson chamber"
- chamber with supersaturated vapor
- droplets formed along trail of ionisation

- 6mm lead plate separating upper and lower chamber
- placed in magnetic field

- proper illumination → photograph
- ➔ momentum measured from radius of curvature

Discovery of positron:
- using cosmic rays
- track enters from below (radius!)
- positive charge (bending direction)
- $Q_{e+} < 2x\ Q_{e-}$
- $M_{e+} < 20x\ M_{e-}$
- out of 1300 photographs 15 with $e^+$

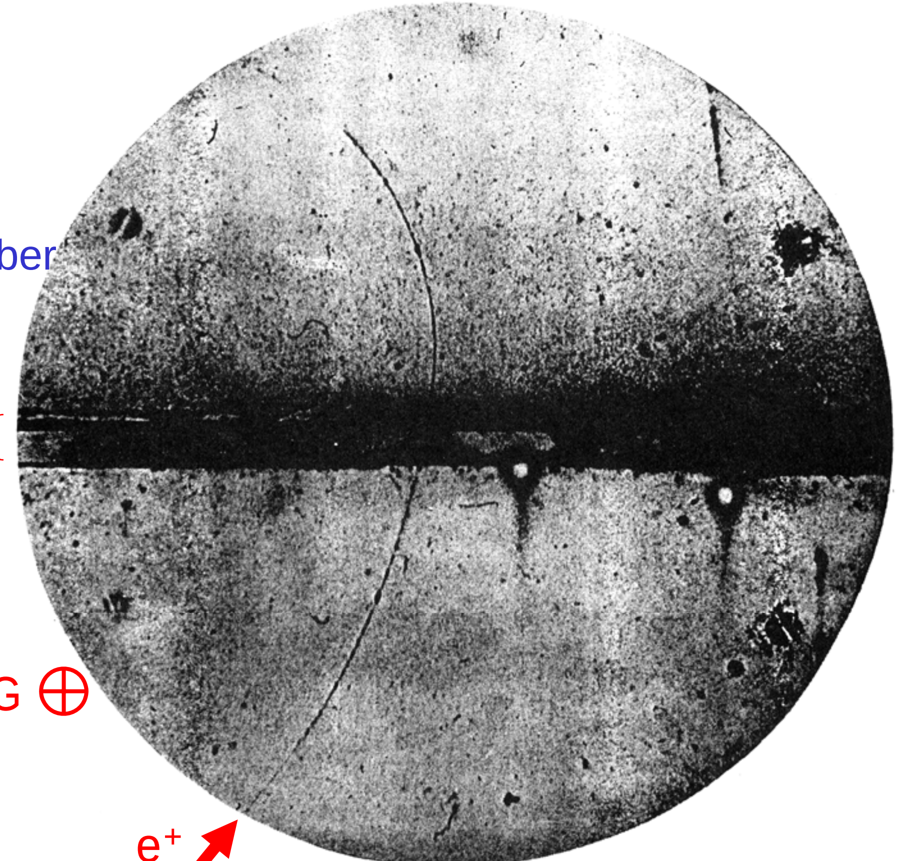


FIG. 1. A 63 million volt positron ($H\rho = 2.1 \times 10^5$ gauss-cm) passing through a 6 mm lead plate and emerging as a 23 million volt positron ($H\rho = 7.5 \times 10^4$ gauss-cm). The length of this latter path is at least ten times greater than the possible length of a proton path of this curvature.

# Cloud Chamber

- stereoscopic photographs
- 5000 photographs / 1500 hours (3.3 per hour)
- 2 with new features …

Rochester & Butler 1947

3cm lead

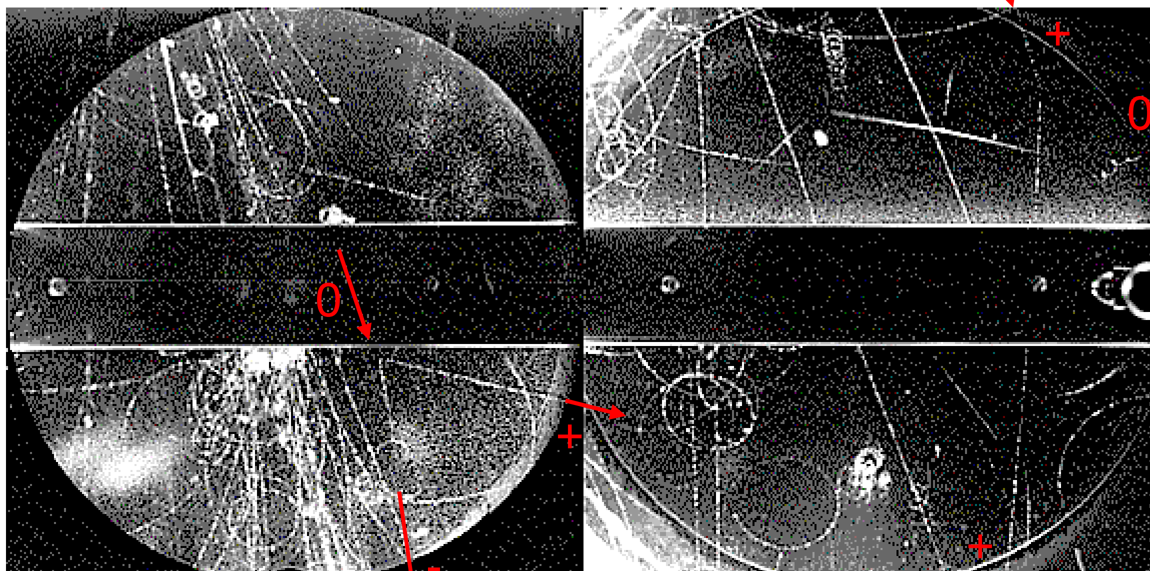


3.5 kG ⊕

7.2 kG ⊕

Discoveries:

- using cosmic rays

- neutral particle decay into two charged
- charged particle decay into charged and neutral

Modern candidates: $K_S^0 \rightarrow \pi^+\pi^-$ $K^+ \rightarrow \pi^+\pi^0$

# Nuclear Emulsion

- emulsion with photographic silver-bromide crystals
- charged tracks give 'latent images' which become visible from standard photo-processing
- single layer: 25-200$\mu$m thick
- several hundred packed in a stack
- correlation via fiducial marks
- 1$\mu$m resolution $\rightarrow$ microscope measurements
- density 3.8 g/cm$^3$ $\rightarrow$ max. energy limited

Lattes, Muirhead, Occhialini, Powell 1947

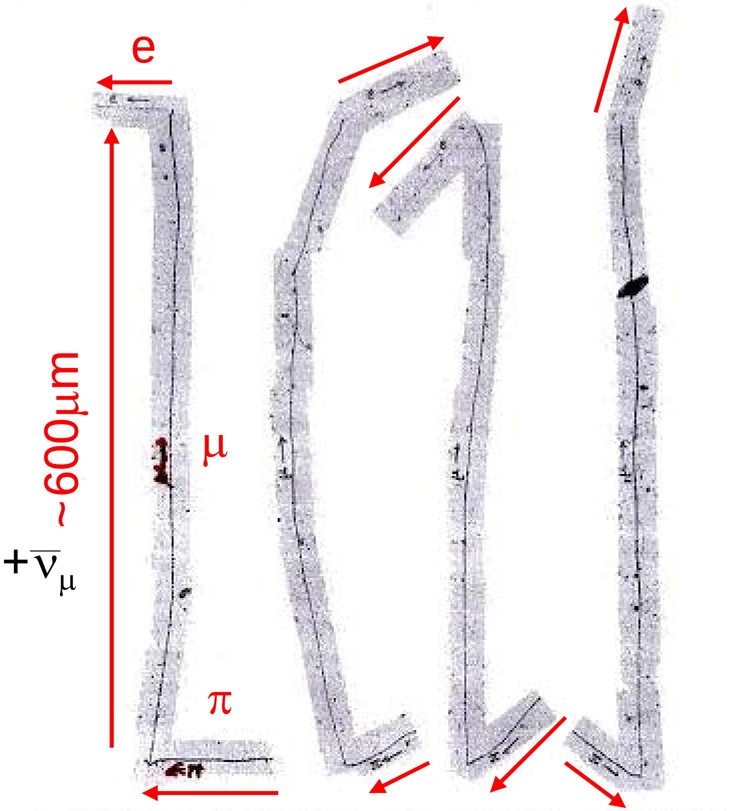


Fig. 1.3 Examples of the decay sequence $\pi^+ \to \mu^+ \to e^+$ in G5 emulsion exposed at Pic du Midi. The constancy of range ($\simeq$ 600 $\mu$m) of the muon implies two-body decay at rest of the pion: $\pi^+ \to \mu^+ + \nu_\mu$. The first examples of pion decay were observed by Lattes, Muirhead, Occhialini, and Powell in 1947. The electron emitted in muon decay, $\mu^+ \to e^+ + \nu_e + \bar{\nu}_\mu$, was not observed in the early experiments employing less sensitive emulsions. (Photograph courtesy University of Bristol).

Modern picture:

$$\pi^+ \rightarrow \mu^+ + \nu_\mu$$
$$\mu^+ \rightarrow e^+ + \nu_e + \overline{\nu}_\mu$$

Discovery of pion decay into muon:
- large ionisation at slow velocity
- decay at rest
- constant muon track length
  - $\rightarrow$ constant energy
  - $\rightarrow$ 2-body decay!
- neutrinos not captured
- electron is relativistic $\rightarrow$ leaves emulsion

# Bubble Chamber

- invented by Glaser in 1952
- filled with liquefied gas at 5-20 atm
- $H_2$,$D_2$, He, $C_3H_8$ ,Ar, Ne, Xe
- close to boiling T
- tracks pass $\rightarrow$ expand volume (1ms)
  - $\rightarrow$ superheating
  - $\rightarrow$ bubbles grow (2ms)
  - $\rightarrow$ relax: bubbles stop growing
  - $\rightarrow$ photograph (stereo, even holographic: HOBC)
- cycle time ~ 1s
- homogeneous field: up to B=2-3.5T
  - $\rightarrow$ track bending ($\int B dl$=10Tm): particle momentum
  - $\rightarrow$ bubble density ~ energy loss dE/dx
  - $\rightarrow$ for P/(mc)<3: mass measurement $m=\sqrt{1-\beta^2}\,P/(\beta c)$
- advantage: great detail in complex reactions
- disadvantage: not usable at collider, energy limited

BEBC, 1976-83

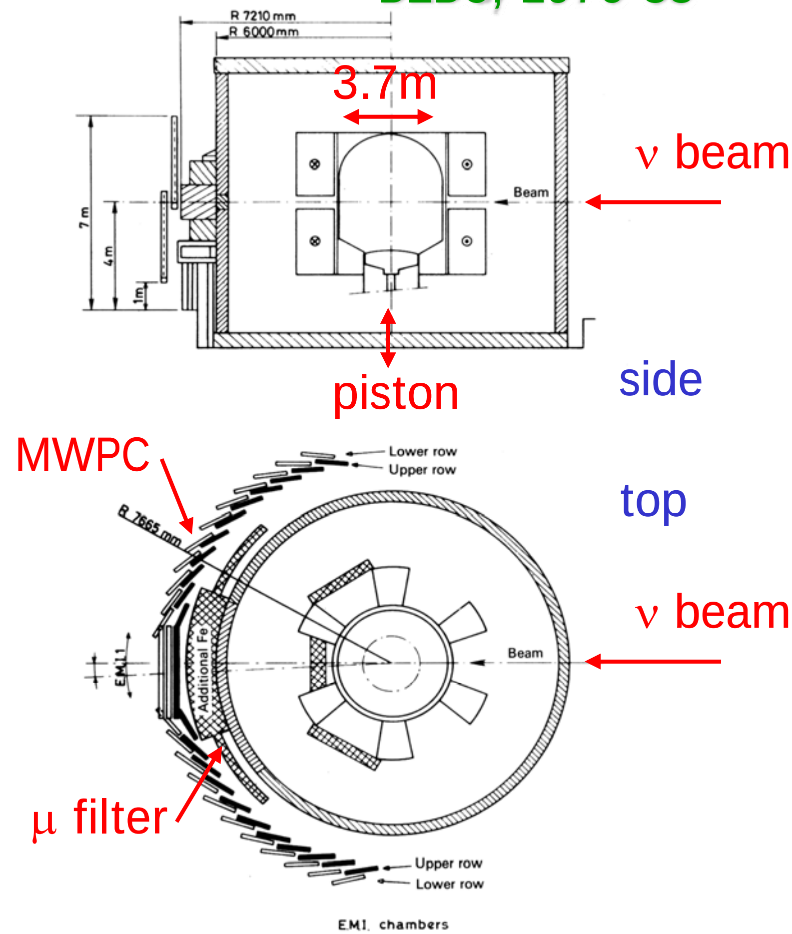


**Figure 2.14** Elevation and plan views of the 3.7-m-diameter bubble chamber (BEBC) at CERN. The chamber is filled with liquid hydrogen, deuterium, or neon-hydrogen mixture and is equipped for neutrino experiments with an external muon identifier. This consists of 150 m² of multiwire proportional chambers placed outside the magnet yoke.

# Bubble Chamber

Powell, Segrè et.al. 1958

Button et.al. 1961

30 inch, propane

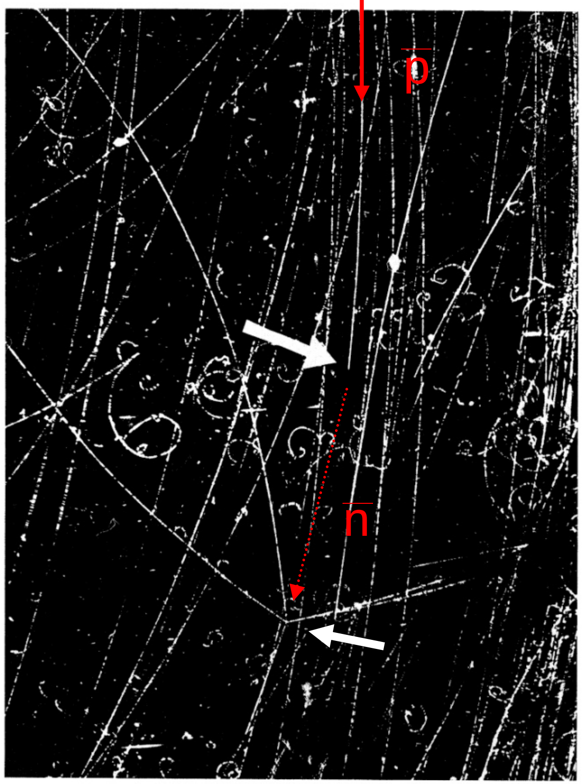


Figure 4.2: An antiproton enters the bubble chamber from the top. Its track disappears at the arrow as it charge exchanges, $p\bar{p} \rightarrow n\bar{n}$. The antineutron produces the star seen in the lower portion of the picture. The energy released in the star was greater than 1500 MeV. (Ref. 4.7)

72 inch, hydrogen

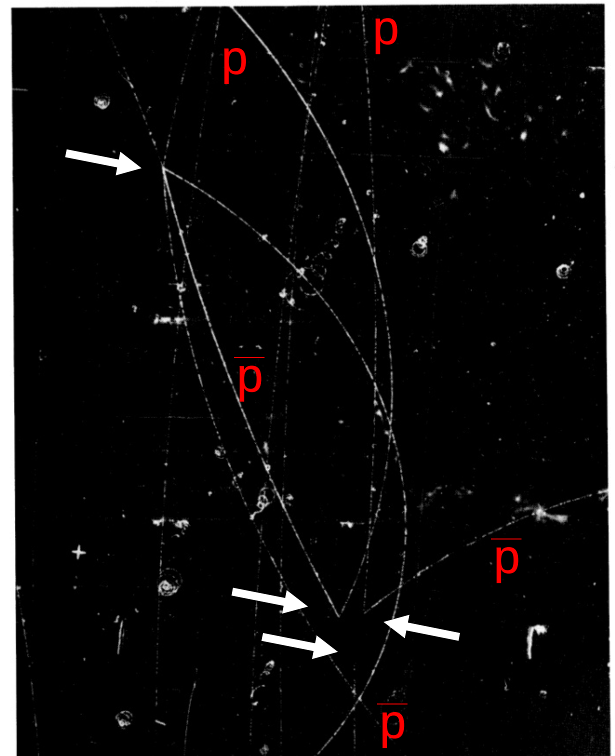


Figure 4.3: Production of a $\Lambda\bar{\Lambda}$ pair by an incident antiproton. The antiproton enters the chamber at the bottom and annihilates with a proton. The $\Lambda$ and $\bar{\Lambda}$ decay nearby. The antiproton from the antilambda annihilates on the left-hand side of the picture and gives rise to a 4 prong star. The picture is from the 72-inch bubble chamber at the Bevatron. (Ref. 4.9)

$p\bar{p} \rightarrow n\bar{n}$ first: Cork, Lambertson, Piccioni, Wenzel, 1956

$p\bar{p} \rightarrow \Lambda\bar{\Lambda}$ first: Prowse, Baldo-Ceolin, 1958

# Bubble Chamber

Samios, Shutt 1964

80 inch, hydrogen

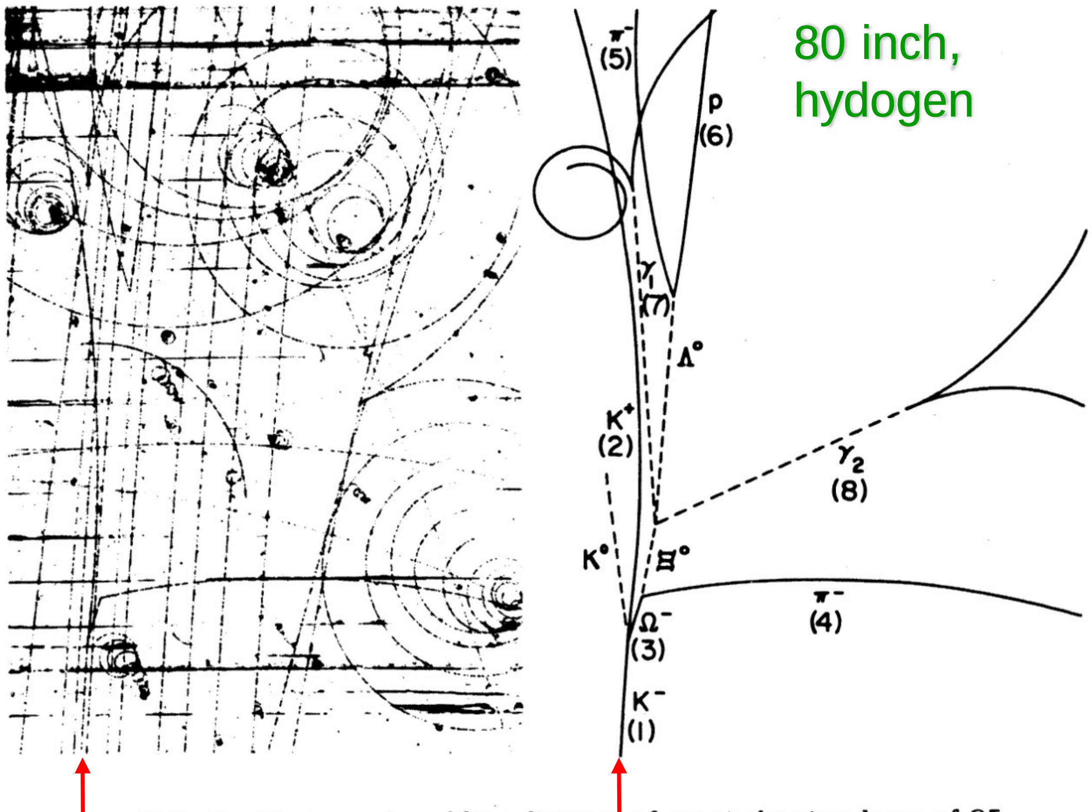


FIG. 2. Photograph and line diagram of event showing decay of Ω⁻.

- $\Omega^-$ production
- $J^P=3/2^+$ decuplet complete

Gargamelle chamber 1973 (-1978)

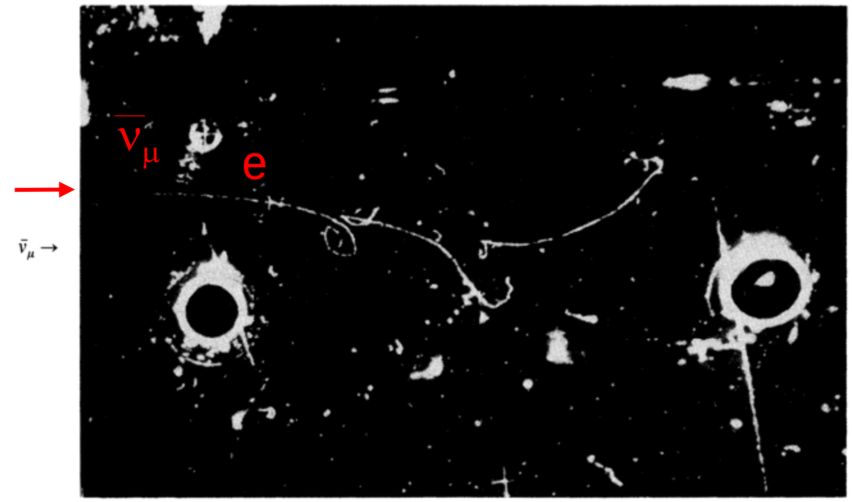


**Figure 1.6** First example of weak neutral-current process $\bar{\nu}_\mu + e \rightarrow \bar{\nu}_\mu + e$ observed in heavy-liquid bubble chamber Gargamelle at CERN irradiated with a $\bar{\nu}_\mu$ beam (Hasert *et al.*, 1973). A single electron of energy 400 MeV is projected at a small angle ($1.5 \pm 1.5°$) to the beam, and is identified by bremsstrahlung and pair production along the track (see Chapter 2). About $10^9$ $\bar{\nu}_\mu$'s traverse the chamber in each pulse and three such events were observed in 1.4 million pictures. (Courtesy CERN.)

$$\bar{\nu}_\mu e \rightarrow \bar{\nu}_\mu e$$

- $E_e$=400MeV, angle: 1.5°± 1.5°
- bremsstrahlung & pair-production
- 3 events / 1.4M pictures, $10^9$ $\nu$/pulse

# Bubble Chamber

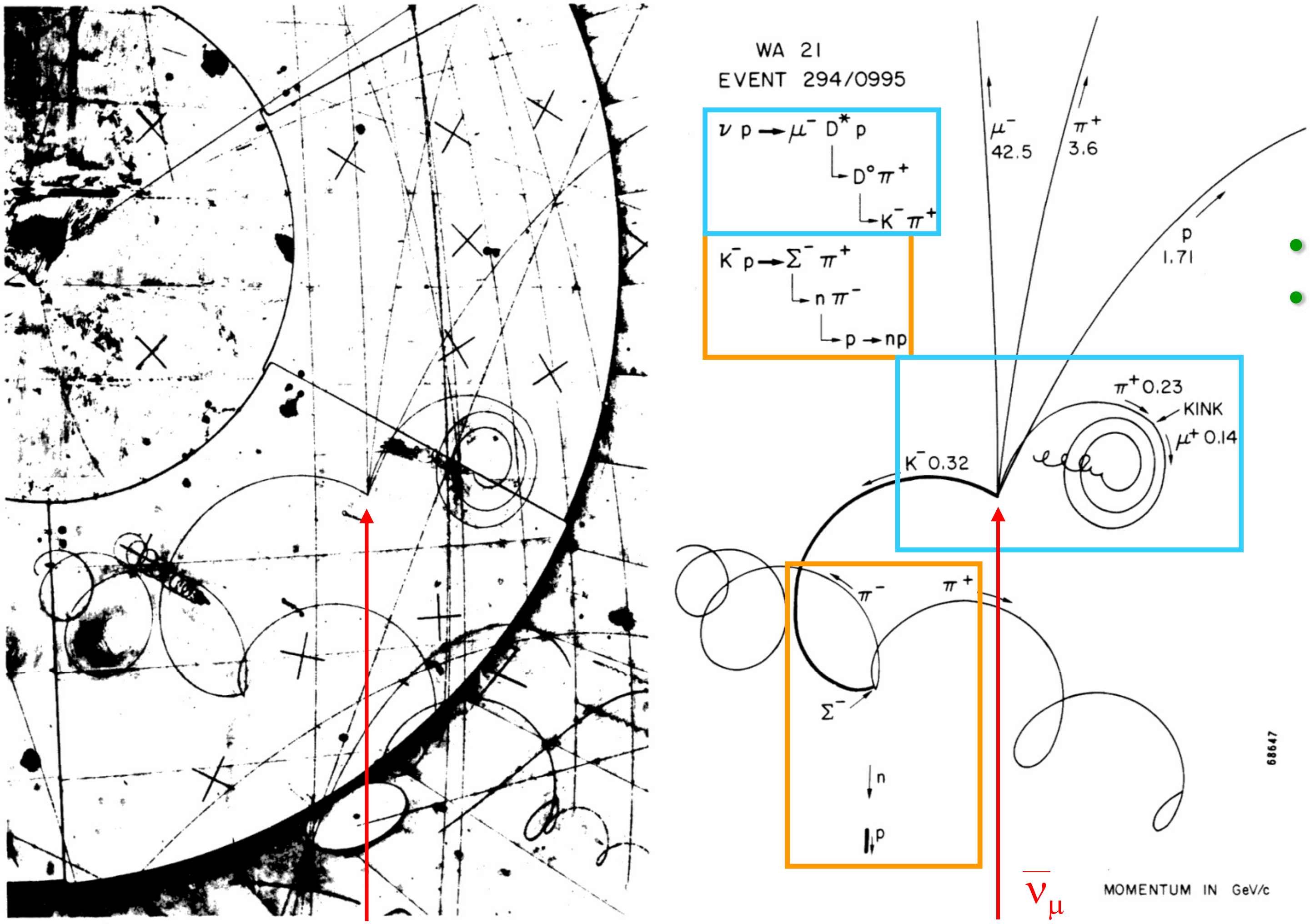


BEBC

- charm production
- ... after 1974 ...

**Figure 2.15** Example of charmed-particle production and decay in the hydrogen bubble chamber BEBC exposed to a neutrino beam at the CERN SPS. (Courtesy CERN.)

# Scintillation Counter

- liquid organic scintillator (here doped by cadmium)

- charged track excites matrix
  - $\rightarrow$ UV light emission (absorption length: few mm!)
  - $\rightarrow$ absorption by fluorescent agent
  - $\rightarrow$ re-emission in the visible
  - $\rightarrow$ photon detection
- time resolution: O(ns)

Cowan, Reines 1956+58

$\overline{\nu}_e$ from reactor

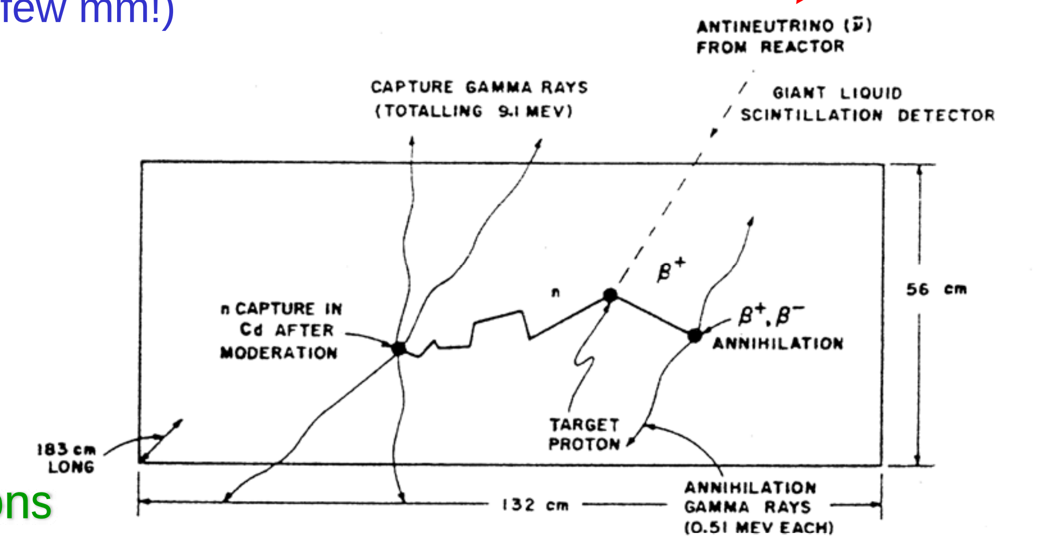


Figure 6.3: A schematic diagram of the experiment of Reines and Cowan in which antineutrinos from a nuclear reactor were detected. The dashed line entering from above indicates the antineutrino. The antineutrino transmutes a proton into a neutron and a positron. The annihilation of the positron produces two prompt gamma rays, which are detected by the scintillator. The neutron is slowed in the scintillator and eventually captured by cadmium, which then also emits delayed gamma rays. The combination of the prompt and delayed gamma rays is the signature of the antineutrino interaction (**Ref. 6.7**).

First neutrino induced reaction:
- inverse neutron decay
- Cd dopant to capture moderated neutrons

$\overline{\nu}_e p \rightarrow e^+ n$

$e^+e^- \rightarrow \gamma\gamma$ prompt

$n\,Cd \rightarrow Cd^* \rightarrow Cd\,\gamma$ delayed

- rate with reactor on higher!!

# Time of Flight

- particle identification through flight time:
  $\Delta t = L/c\,(1/\beta_1 - 1/\beta_2)$,   $P = m\,\gamma c$
- time resolution: $\sigma_t = 0.3$ns
  (organic scintillation counter)
- $4\sigma_t$ separation:
  $\pi$-K @ 1GeV needs 3.4m flight path
  e-$\pi$ @ 200MeV needs 1m flight path
- method limited to low momenta (<2GeV/c)

SLAC-LBL MARK I 1974

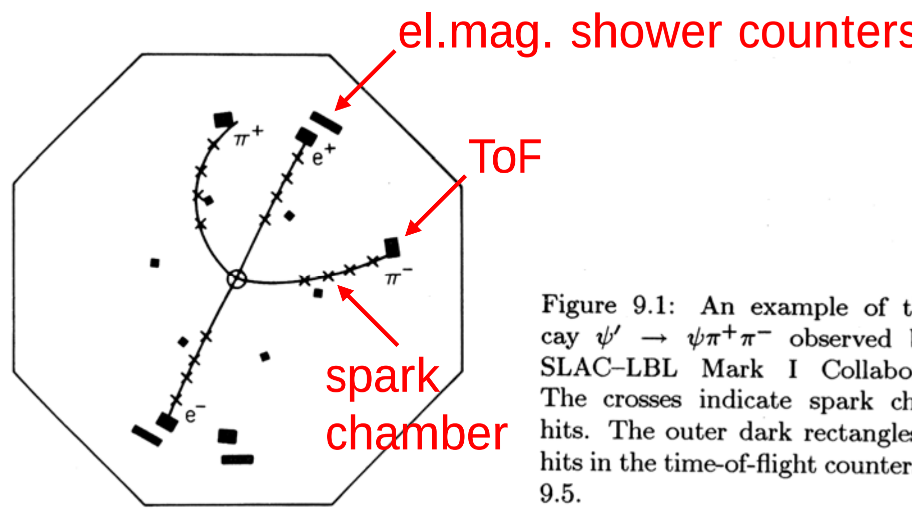


Figure 9.1: An example of the decay $\psi' \to \psi\pi^+\pi^-$ observed by the SLAC–LBL Mark I Collaboration. The crosses indicate spark chamber hits. The outer dark rectangles show hits in the time-of-flight counters. Ref. 9.5.

10 days after 'November revolution':
(discovery of J/$\Psi$)

- discovery of $\Psi^*$
- subsequent discovery of decay $\Psi^* \to \Psi\pi^+\pi^-$
- $\pi$ identification possible due to their low momentum (150MeV)

$\Psi^* \to \Psi\pi^+\pi^-$   $\pi$: 150MeV

$\Psi \to e^+e^-$   e: 1.5GeV

# Cherenkov Counter

- particle identification through velocity measurement:
- charged particle: $\beta c = v > c/n$
- 'shock-wave': coherent wave front with angle

  $\cos \Theta_C = 1/\beta n(\omega)$

  (+ finite radiator effects)
- ➔ directed photon signal
- use: p=mv
- concepts:
  - threshold counter
  - differential counter
  - ring imaging

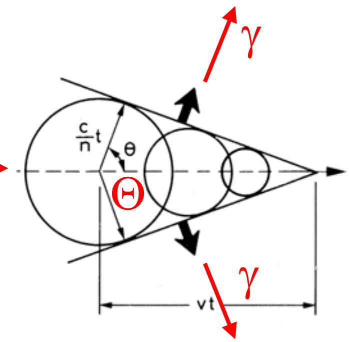


Fig. 5.11. Velocity distribution of charged hyperons with 15 GeV/c momentum in a short secondary beam [LI 73].

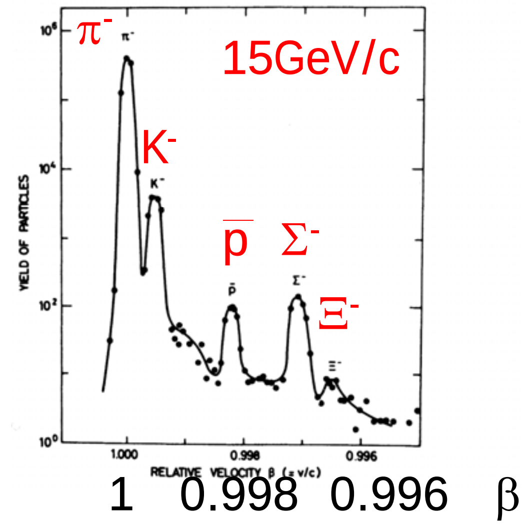


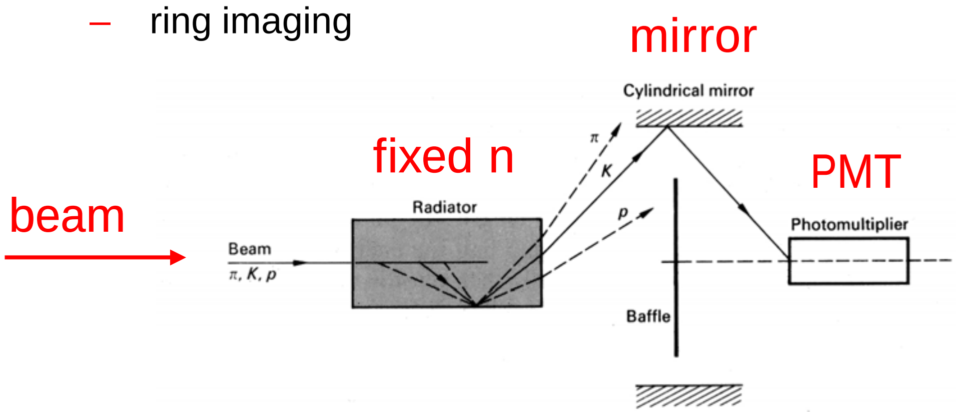


Figure 2.18 Early design of differential Čerenkov counter. The arrangement is intended to select light from one of three components of the beam (K-mesons, in the case shown).

'Cherenkov spectroscopie'

Fig. 5.12. Differential Cherenkov counter with fixed diaphragm and change of refractive index by pressure variation [BO 83].

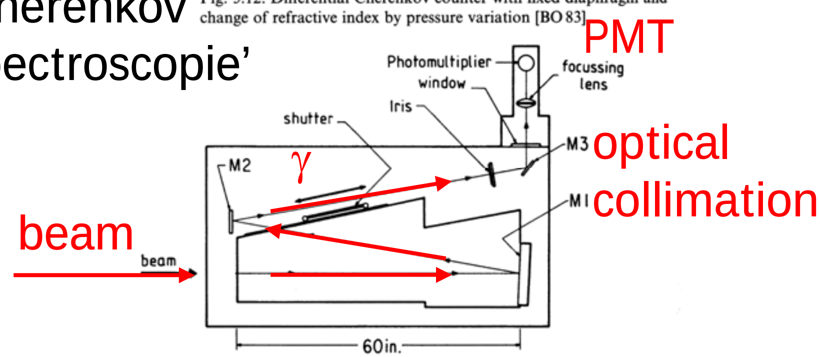


variable pressure: n(P)

# Gaseous Ionisation Counters

- ionisation in (noble) gas volume
- electrostatic field to separate electrons and ions

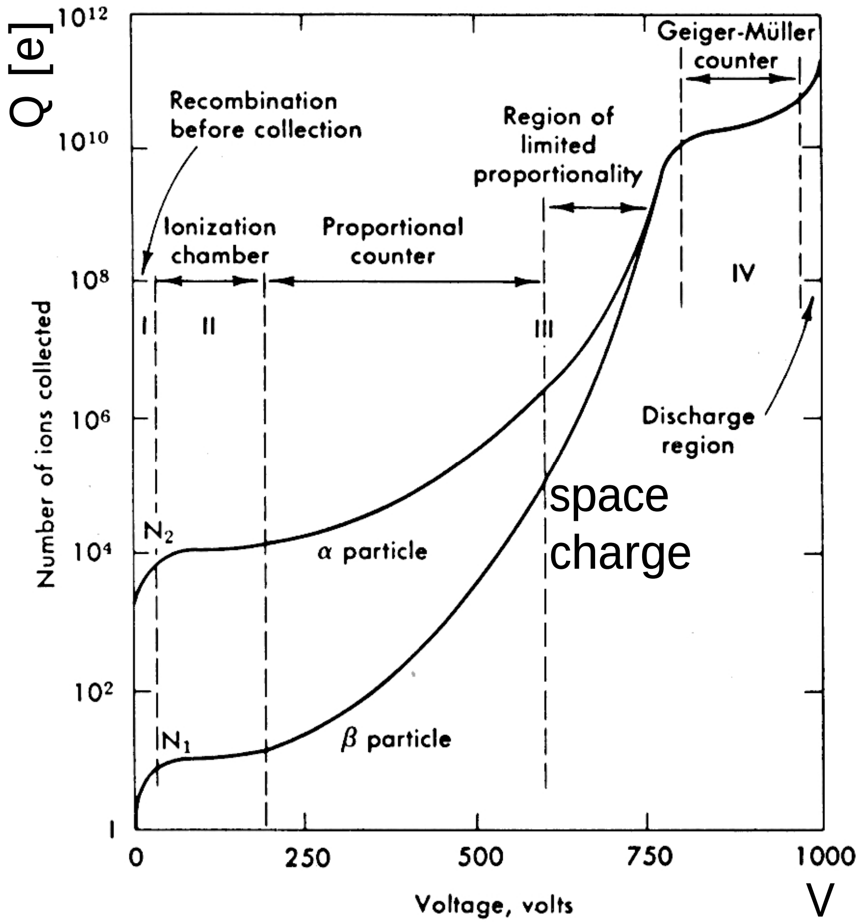


**Fig. 6.2.** Number of ions collected versus applied voltage in a single wire gas chamber (from *Melissinos* [6.1])

- Ionisation chamber
  - collect (small) charge
- Proportional counter
  - avalanche from secondary ionisation
  - gain up to $10^6$
- Geiger-Müller counter
  - chain reaction of avalanches, needs quenching
  - saturated output

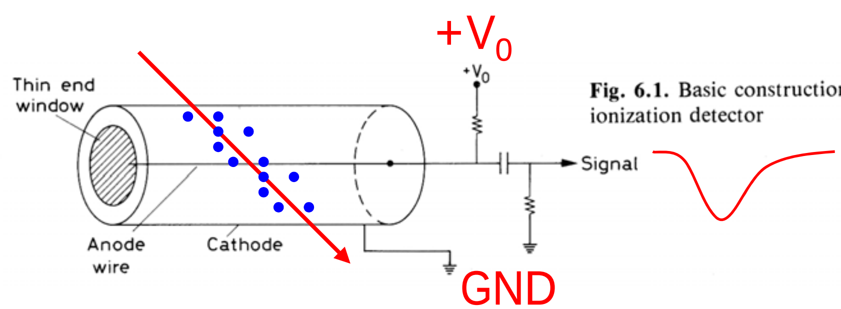


**Fig. 6.1.** Basic construction of a simple gas ionization detector

# Spark Chamber

- planar electrodes with noble gas filling
- alternate connection to pulsed HV (E>20kV/cm) and GND
- charged particle passes
- trigger turns field on
- e-avalanches & streamers are formed → spark
- reach electrodes in ~10ns
- spark discharge photographed or electronically registered

Fig. 3.36. Detection efficiency of a spark chamber as a function of the time delay between the passage of the particle and the application of the high-voltage pulse to the chamber electrodes; the parameter labelling the curves is the voltage used for clearing the chamber after a spark [CR 60].

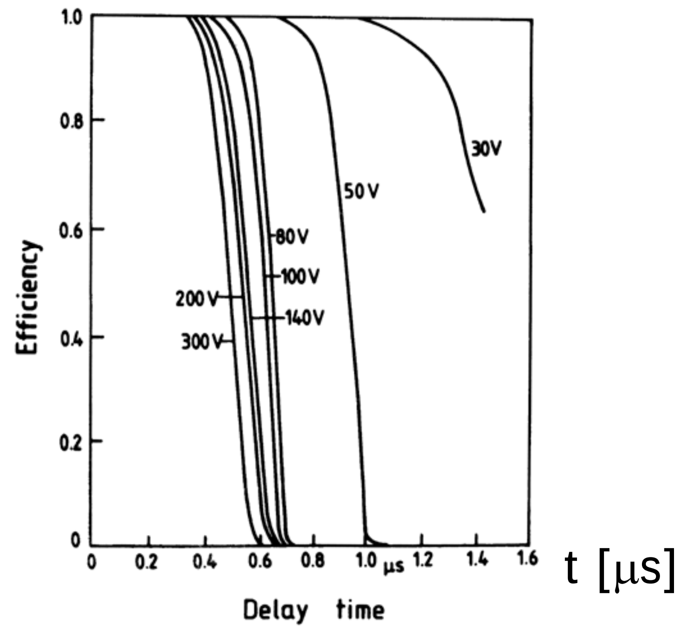


Fig. 3.35. Principle of the spark chamber. PM, photomultiplier; F, pulse shaper; C, coincidence unit; V, amplifier; SG, spark gap. The arrow shows the path of an ionizing particle.

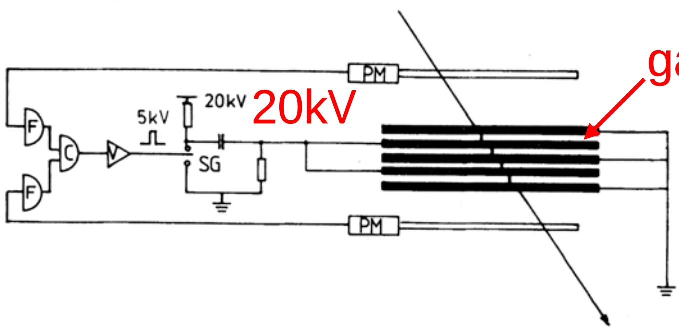


- inverted static clearing field: to remove generated charge between discharges → dead time up to 100μs
- efficiency depending on time delay and clearing field
- dead time for HV pulser recharge: 1-10ms

# Spark Chamber

First evidence for two neutrinos:

- 15GeV protons from AGS on Be target

$$\pi \to \mu\nu$$

- $\mu$ shielded by 13.5m iron wall
- 10 ton spark chamber (Al plates)
- $\mu$-appearance with E>300MeV:

34: $\nu n \to p\mu^-$ or $\bar{\nu} p \to n\mu^+$

22: $\nu n \to n\pi^+\mu^-$ or $\nu n \to p\mu^-$

8: shower-like (unlikely due to $e^-$)

- conclusion: $\nu_\mu$ and $\nu_e$ exist!!

Schwatz, Ledermann, Steinberger 1962

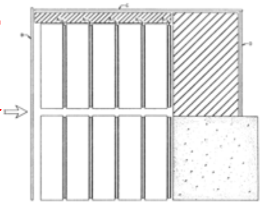


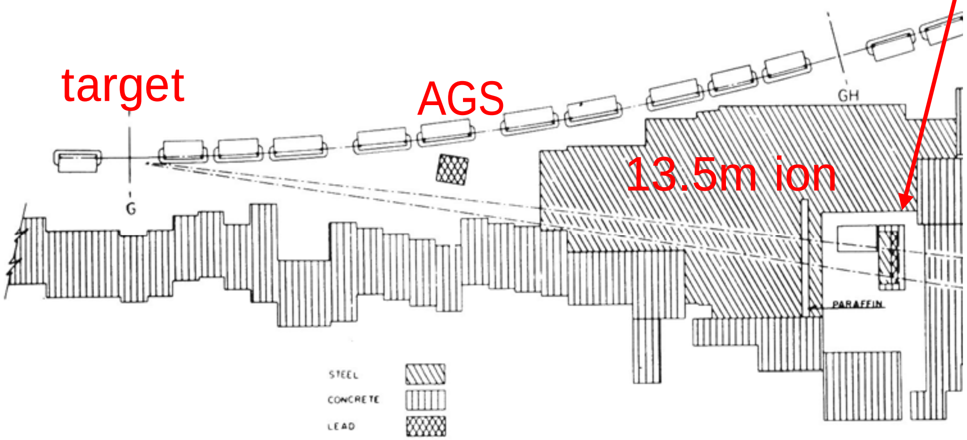


FIG. 1. Plan view of AGS neutrino experiment.

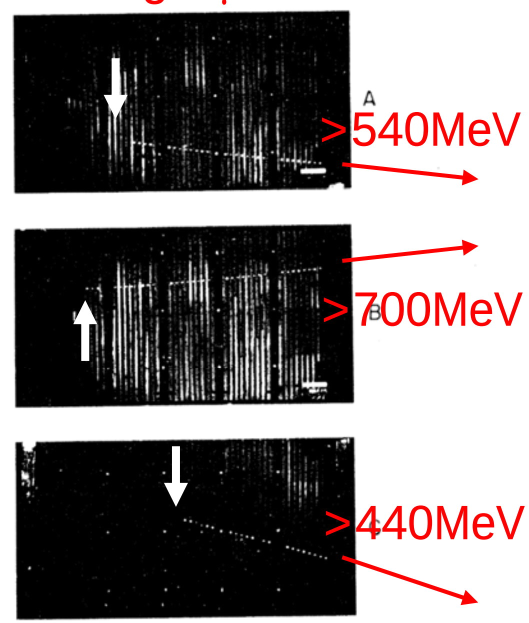


FIG. 5. Single muon events. (A) $p_\mu > 540$ MeV and $\delta$ ray indicating direction of motion (neutrino beam incident from left); (B) $p_\mu > 700$ MeV/$c$; (C) $p_\mu > 440$ with $\delta$ ray.

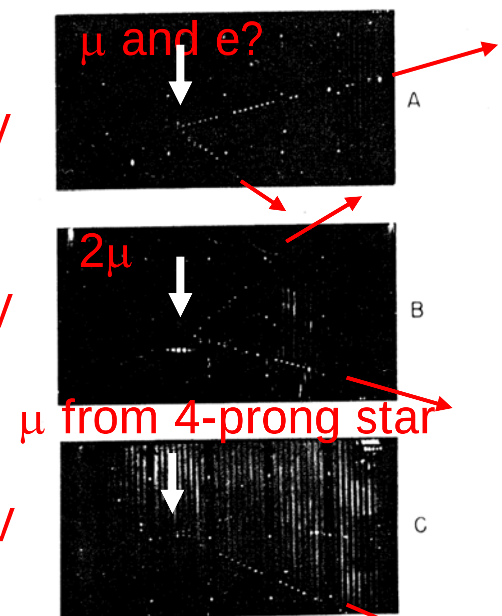


FIG. 6. Vertex events. (A) Single muon of $p_\mu > 500$ MeV and electron-type track; (B) possible example of two muons, both leave chamber; (C) four prong star with one long track of $p_\mu > 600$ MeV/$c$.

# Streamer Chamber

- planar electrodes with noble gas filling
- charged particle passes
- trigger switches strong, short field, ⊥ to track:
  E>40kV/cm for ~1ns
- generates e-avalanches: gas amplification >$10^8$
- short discharge channels: 0.2-1mm

Fig. 3.32. Spatial development of a streamer in a time sequence from left to right [AL 69].

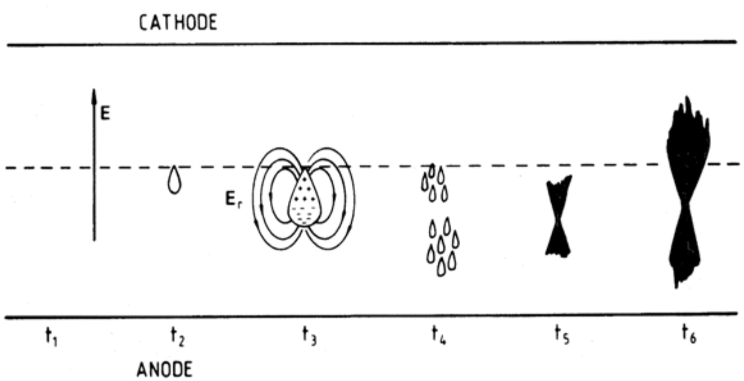


- extremely good space resolution:
- Yale chamber: E>330kV/cm for 0.5ns → resolution: 32μm
  used e.g. in charmed particle lifetime studies ($10^{-13}$s)

Fig. 3.31. Principle of streamer chamber (schematic).

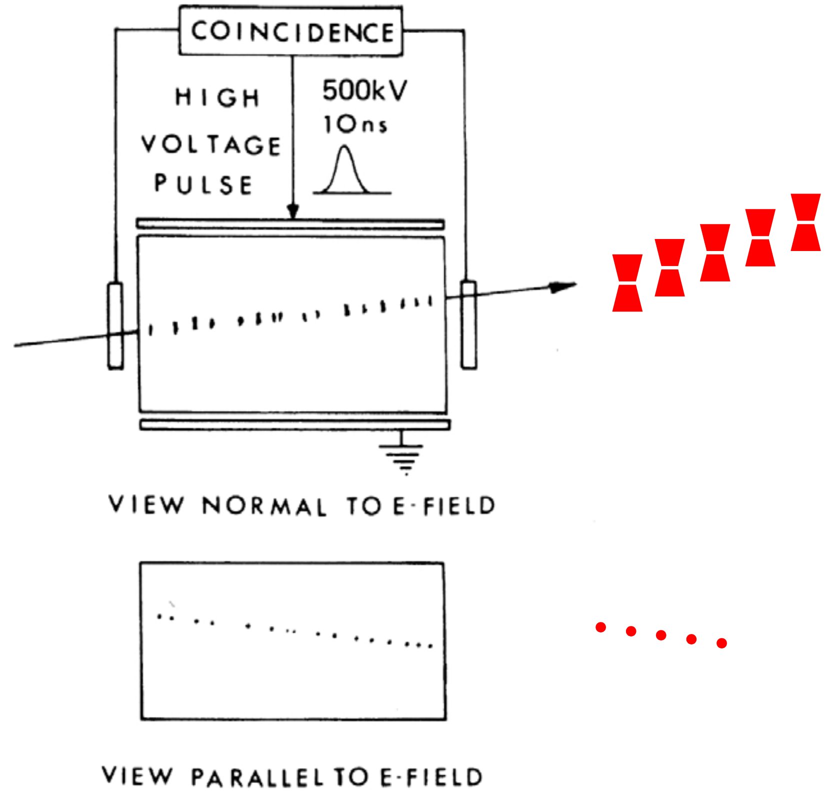

# Streamer Chamber

NA5 1980

Fig. 3.33. Interaction of a $\pi^-$ meson at 300 GeV energy in a liquid hydrogen target. The tracks of the reaction products are recorded in a streamer chamber of dimensions $200 \times 120 \times 72\,\mathrm{cm}^3$ [EC 80].

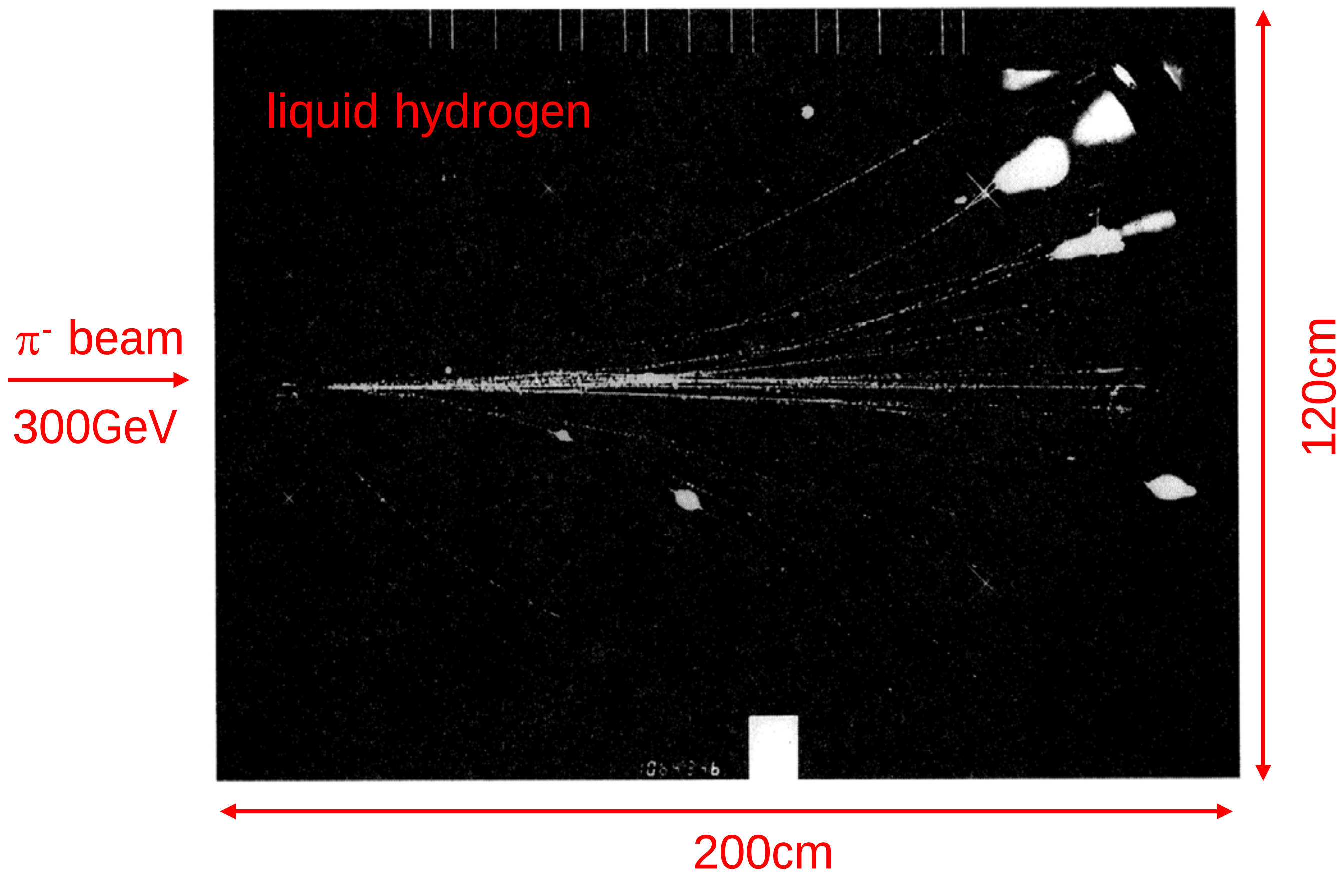

# Early Spectrometers

precise measurement of $\pi$ masses:

$\pi^- p \rightarrow \pi^0 n$

$\pi^0 \rightarrow \gamma\gamma$

$\pi^- p \rightarrow \gamma n$

- $m_\pi = 275.2 \pm 2.5\ m_e$
- $m_{\pi^-} - m_{\pi^0} = 10.6 \pm 2.0\ m_e$

determination of quantum numbers:

$\pi^- d \rightarrow nn$ seen (inferred from $\pi^- p$)

$\pi^- d \rightarrow nn\gamma$

$\pi^- d \rightarrow nn\pi^0$ not seen

- from symmetries:
- $\pi$ is vector
- $\pi^-$ and $\pi^0$ have same parity

Panofsky, Aamodt, Hadley 1951

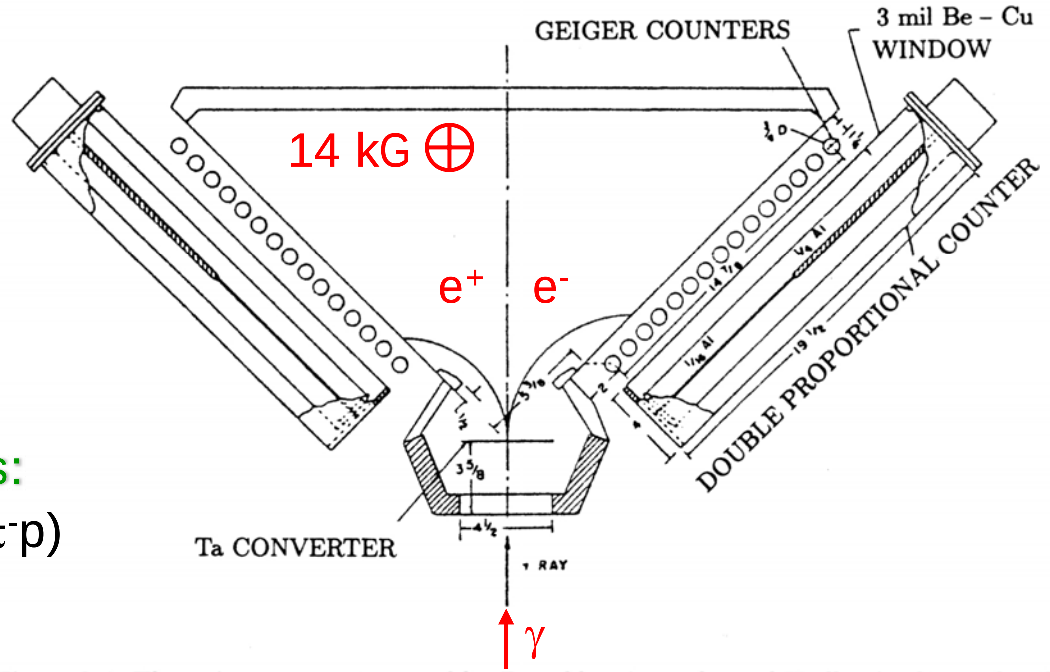


Figure 2.4: The pair spectrometer used by Panofsky, Aamodt, and Hadley in the study of $\pi^- p$ and $\pi^- d$ reactions. A magnetic field of 14 kG perpendicular to the plane shown bent the positrons and electrons into the Geiger counters on opposite sides of the spectrometer. (Ref. 2.9)

# Early Spectrometers

elastic ep scattering → structure function

- form factor:
  $F(q^2) = \int d^3r \exp(i\, q{\cdot}r)\, \rho(r)$
  $\quad\quad = 1 - q^2/6 \langle r^2 \rangle + \ldots$
- $\langle r^2 \rangle = 0.74 \pm 0.24$ fm
- 'root-mean-square charge radius'

McAllister, Hofstadter 1956

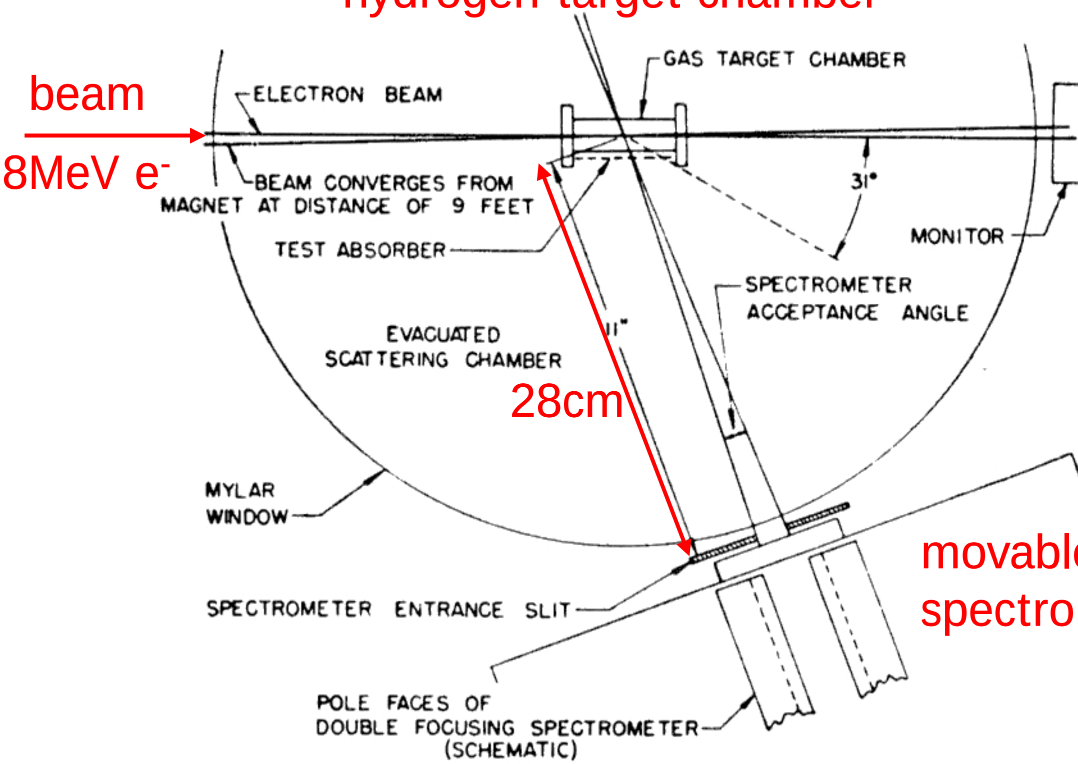


FIG. 2. Arrangement of parts in experiments on electron scattering from a gas target.

measuring structure functions in inelastic scattering became big business in the late 60's, early 70's

- $d\sigma/d\Omega dE = f(F_1(q^2), F_2(q^2), \ldots)$
  or
- $e^{\pm}p$, $e^{\pm}n$, $e^{\pm}d$, $\overset{(-)}{\nu}p$, $\overset{(-)}{\nu}n$, $\overset{(-)}{\nu}d$, …

# Early Spectrometers

Christenson, Cronin, Fitch, Turlay 1964

spectrometer uses:
- spark chambers
- magnet
- scintillator
- water Cherenkov

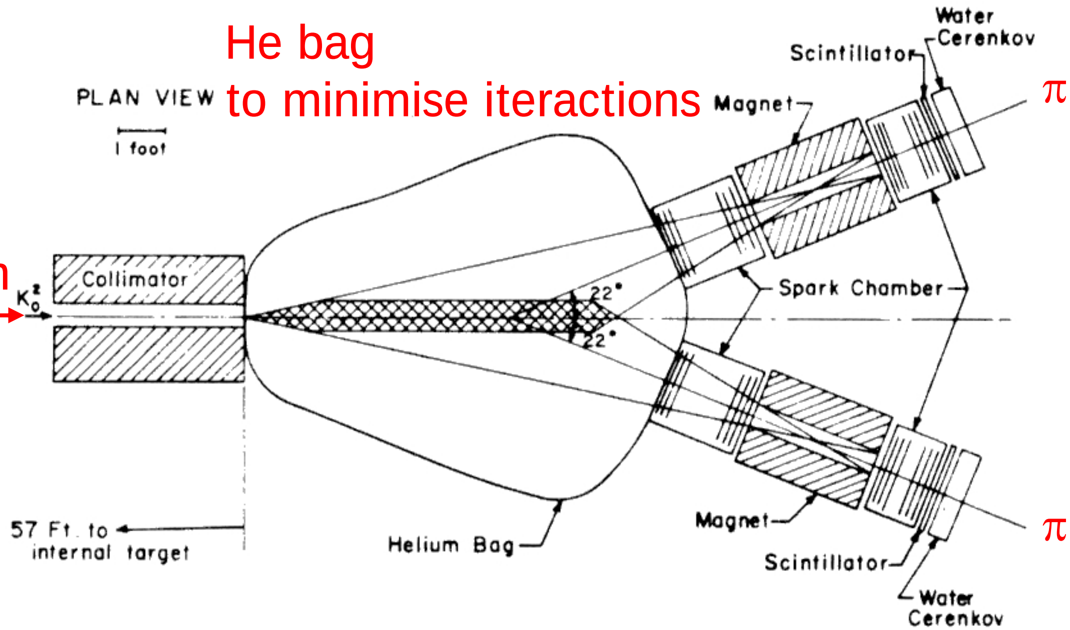


FIG. 1. Plan view of the detector arrangement.

first observation of: $K^0_L \rightarrow \pi^+\pi^-$
- forbidden if CP symmetry is good

- but found: BR = $2\text{x}10^{-3}$

- so in fact: $|K^0_L\rangle = |K^0_2\rangle + \varepsilon|K^0_1\rangle$
  with $|K^0_1\rangle$ CP even $\rightarrow 2\pi$
  $|K^0_2\rangle$ CP odd $\rightarrow 3\pi$

# Detector Concepts

- Single technology detectors:
  - cloud chamber
  - bubble chamber
  - nuclear emulsion
  - liquid scintillator
  - spark/streamer chamber
- Spectrometers:
  - double arm, fixed angle
  - single arm, movable
  - combine tracking, energy measurement, triggering and vetoing
- Signal sources:
  - cosmic rays
  - reactors
  - accelerators - fixed target
  - accelerators with beam-beam interactions

- Drive to develop detectors which:
  - cover more phase space
    - solid angle
    - energy range
  - provide better resolution
    - position
    - momentum
    - energy
    - time
  - measure more parameters simultaneously
    - integration of technologies
  - acquire data faster / more automated
    - electronics development
    - trigger

➔ General purpose detector: the “egg-laying wool-milk-pig”

➔ you always fight: money, manpower, space, time

# Quark Confinement

- Poses an additional Dilemma:
  - Theory predicts distributions for quarks and partons to:
    - Leading Order (LO)
    - Next-to Leading Order (NLO)
    - Next-to-Next-to Leading Order (NNLO)
    - Leading Logarithms (LL)
    - Next-to Leading Logarithms (NLL)
  - Experiment/detector measures hadrons

- Hadronisation not well understood:
  - theorists develop phenomenological descriptions
    - PYTHIA, HERWIG
  - experimentalist resort to Monte Carlo methods using these hadronisation models and knowledge about particle interaction with matter to predict the detector response

# Underlying Physics...

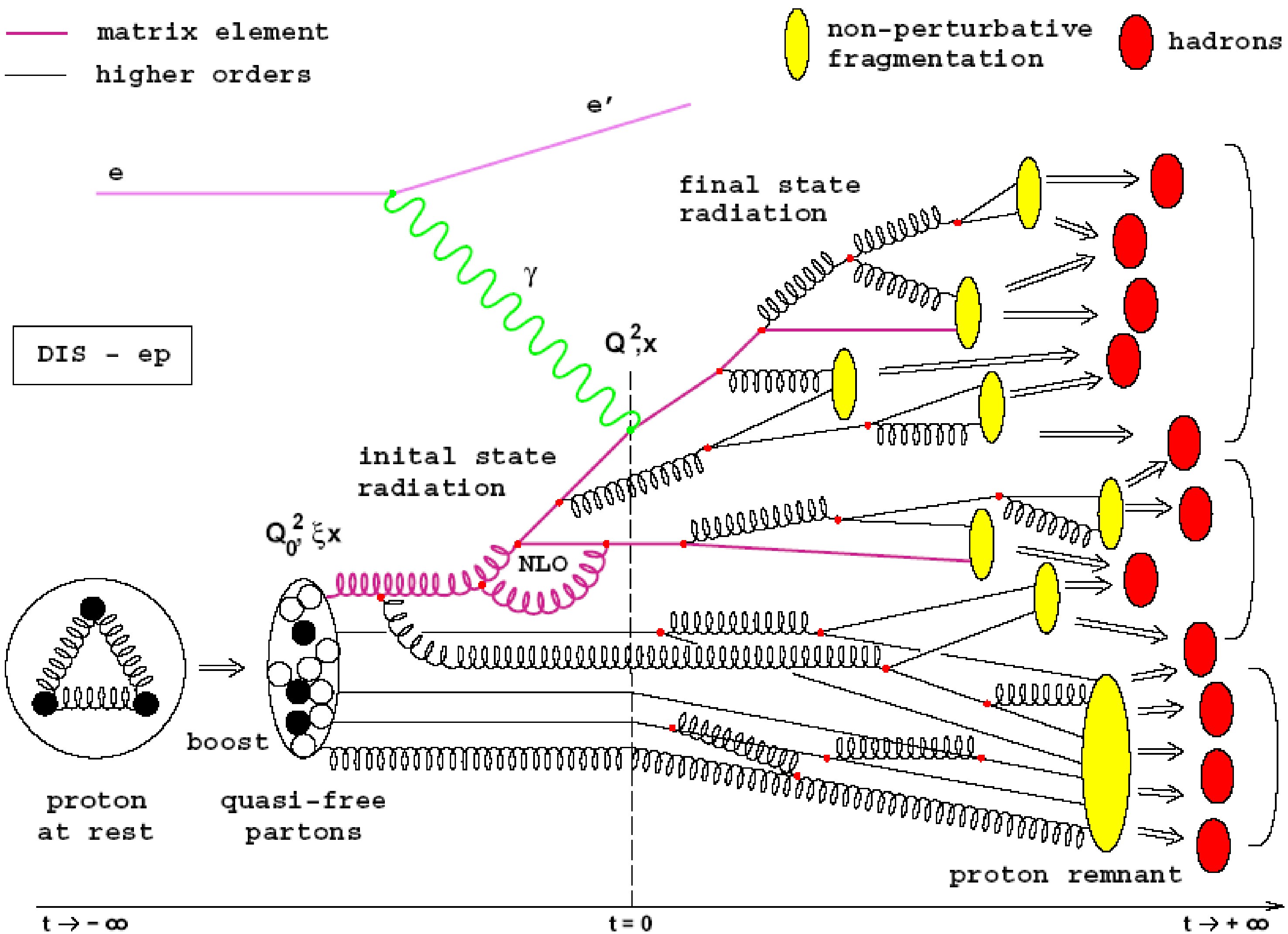

# ...Traces in Detector